Journal of Applied Sciences

ISSN 1812-5654

science alert

ANSInet
an open access publisher
http://ansinet.com

Journal of Applied Sciences 11 (15): 2700-2711, 2011
ISSN 1812-5654 / DOI: 10.3923/jas.2011.2700.2711

Covalent Functionalization for Multi-walled Carbon Nanotube (f-MWCNT)-Folic Acid Bound Bioconjugate

[1]Jacob M. Ngoy, [2]Sunny E. Iyuke, [1]Wilhelm E. Neuse and [2,3]Clarence S. Yah
[1]School of Chemistry, University of the Witwatersrand, Johannesburg,
Private Bag 3, Wits 2050, South Africa
[2]School of Chemical and Metallurgical Engineering, University of the Witwatersrand,
Johannesburg, Private Bag 3, Wits 2050, South Africa
[3]Department of Biochemistry and Toxicology, National Institute for Occupational Health (NIOH),
25 Hospital Street, Constitutional Hill, Johannesburg, South Africa

Abstract: In the current concept, covalently functionalized multi-walled carbon nanotube (MWCNT) as a bioconjugate to folic acid (FA); an essential, bioavailable water soluble B-complex vitamin which is usually expressed on the surfaces of most tumoral cells was used. This was rendered possible through the design of a bioreversible binding water-soluble and biocompatible functionalized multi-walled carbon nanotubes (f-MWCNTs). The MWCNT was synthesized through the Chemical Vapor Deposition (CVD). The MWCNTs were covalently functionalized with sulphuric and nitric acids (3:1) at Room Temperature (RT), 50 and 100°C to generate the phenol and carboxyl groups. Furthermore, aspartic acid at 230°C was used to generate the carboxyl f-MWCNTs groups. The CNTs and f-MWCNTs were both characterized with the aid of a Transmission Electron Microscopy (TEM). The results showed a decreased in mol ratio (COOH/OH) of the f-CNTs from 80 to 20 nm as the temperature increases from RT to 100°C. The f-CNTs carboxyl were attached to 3-(N, N-dimethylamino) propylamine (DMP) and FA through 2-(1H-benzotrial-1-yl)-1, 1,3,3-tetramethylurium hexafluorophosphate (HBTU) to generate f-CNTs-FA conjugates. The results of the high resolution nuclear magnetic resonance (H^1NMR) and infrared (IR) spectra showed CONH peak shifts bond bioreversible conjugation of FA at 94 and 101.3% and sizes 50 and 170 nm, respectively. The f-MWNT-FA moieties thereby have a greater versatility and can be used for the treatment and restoration of neoplasma cells.

Key words: Functionalized multi-walled carbon nanotubes, functionalized carbon nanotubes folic acid, bioconjugates, nanocomposites

INTRODUCTION

The search for new and effective drug delivery systems is a fundamental principle to design and improve pharmacological and therapeutic profile of drug molecules (Allen and Cullis, 2004; Fekri *et al*., 2010; Alkhatib *et al*., 2010; Singh *et al*., 2011; Warisnoicharoen *et al*., 2011). Furthermore, a wide variety of drug delivery systems are currently in existence (Pouton and Seymour, 2000). Current reports by Ke *et al*. (2007) showed polymer-functionalization CNTs as another important polymeric carbon nanocomposites delivery system. This covalent technique allows the combination of different polymers with the CNTs to create new compound classes with wide range of properties (Semwal *et al*., 2010). To achieve this, it is therefore essential to functionalize the CNTs with ideal polymers. Furthermore f-CNT can ease their penetration into the cells, thus offering f-CNT as vehicles for drug delivery (Pantarotto *et al*., 2004; Kam *et al*., 2004). In fact f-CNT can carry one or more therapeutic agents with recognition capacity, optical signal imaging and/or specific targeting, to treat diseases (Ferrari, 2005). For this purpose a new strategy for the multiple functionalization of CNT with different types of molecules (Wu *et al*., 2005) has been developed to ease disease treatment.

Pristine carbon nanotubes have high hydrophobic thus making them insoluble in aqueous solutions. Apart from that they very conducive for the construction of various electrochromic devices, depending on the specific applications in need (Zambri *et al*., 2011).

The problem of insolubility or hydrophobicity can be achieved by functionalization which is the attachment of

Corresponding Author: Sunny E. Iyuke, School of Chemical and Metallurgical Engineering, University of the Witwatersrand, Johannesburg, Private Bag 3, Wits 2050, South Africa

functional groups on the surfaces of CNTs. For biomedical applications, surface chemistry or functionalization is required to solubilize CNTs, thereby rendering them biocompatible and low toxicity. Functionalization generates functional groups at the surfaces of CNTs that react with other chemicals, prepolymers and polymers, thus giving rise to a homogeneous dispersion or solubilization of CNTs. Chemical reactions perform bonds on nanotube sidewalls resulting into covalency properties. These covalencies can be created by chemical oxidation with oxidizing agents such as nitric acid, sulfuric acid and potassium permanganate (Niyogi *et al*., 2002; Rosca *et al*., 2005; Zeng *et al*., 2008). Others include 1, 3-dipolar cycoaddition with methine yides in the presence of N, N-dimethyl formamide. During the process of functionalization, carboxyl groups are formed at the ends and sidewalls of tubes. This type of functionalization generates mainly the −OH and −COOH functional groups. Further attachments can be made on the functional groups, thus increasing their solubility in organic solvents (Xie *et al*., 2002). The carboxylic acid groups often connect the CNTs with the amino-terminated sites present on the biomolecules. During covalent modification, the carboxylic acids are usually activated by thionyl or oxalyl chloride, carbodiimides or active esters, to obtain highly reactive intermediate groups capable of linking the biomolecules and CNTs in the presence of 2-(1H-benzotrial-1-yl)-1,1,3,3-tetramethylurium hexafluorophosphate (HBTU). The covalent attachment assures the hydrophilic properties of CNT.

Further, other anticancer therapies are well-known for their potency to cure autoimmune disease (Wong, 2005). However, most do suffer from low bioavailability and toxic side effects (Pignatello *et al*., 2004). Therefore, an increased bioavailable targeted delivery agent is highly desirable. However, most drugs require high dose concentrations due to their low cellular uptake (Pignatello *et al*., 2001). With functionalization bioavailable low dose concentration, low toxicity drug targeting agents are possible (Pastorin *et al*., 2006). Preliminary findings have shown that Methotrexate (MTX) an anti-cancer drug when conjugated to CNT, its potency increases by 10 times in cell culture (Prato *et al*., 2008). The problem faced is the formation of an amide bond between the MTX and the CNTs reducing its efficacy. The problem however, can be overcome by the introduction of a cleavage linker or an enzymatically sensitive bond as demonstrated in dendrimers conjugates (Quintana *et al*., 2002). The application of FA- CNT conjugates as targeting moiety may render more efficacious translocation to cancerous cells.

Folic acid conjugated CNTs on the other hand have been found necessary to operate as receptor for targeting moiety during the uptake. Passive targeting approaches are limited in their scope and thus, tremendous effort has been directed towards the development of active approaches for drug targeting. Active targeting employs specific modification of drug/drug-carrier nanosystems with active agents having selected affinity for recognizing and interacting with the specific cell, tissue or organ question (Vasir *et al*., 2005). Direct coupling of drug to targeting ligand, restricts the coupling capacity to a few drug molecules. In contrast, coupling of drug carrier nanosystems to ligands allows import of thousands of drug molecules by means of one receptor targeted ligand. Therefore, the current research was aimed at coupling MWCNT with folic acid which can be used as a biocompatible molecule in the improvement of cancer treatment.

MATERIALS AND METHODS

Chemicals: The hydroxyamines and diamines were of analytical grade obtained from Adrich Chemie, Fluka AG, South Africa. Other solvents and reagents obtained from Adrich Chemie, Fluka AG, South Africa include: D,L aspartic acid, phosphoric acid, 3-Dimethylamino-1-Propylamide (DMP), Diethylenetriamine (DET), 2-2-(Ethylenedioxy)-Diethylamine (EDDA), 1,3 Diaminopropane (PDA), Dicyclohexylcarbodiimide (DCC), 2-(1H-Benzotriazol-1-yl)-1,1,3,3-Tetramethyluronium Fluorophosphates (HBTU), Triethylamine (TEA), ferrocene, folic acid, methotrexate, sodium hydroxide, Calcium chloride, chloridric acid, folic acid glacial acetic acid, ammonium hydroxide, sulphuric acid and nitric acid. Distilled water was used for all preparative work. The reaction solvent, N,N-Dimethylformamide (DMF), was distilled under reduced pressure with a fore-runs of around 10% being discarded and was dried over molecular sieves 4 Å. All other solvents, Diethyl ether (Et_2O), hexane, acetone and toluene were of laboratory grade, received from Adrich Chemie, Fluka AG, South Africa. The acetylene, argon and nitrogen gases were also of analytical grade obtained from Afrox South Africa for the CNT production.

The production multi-walled carbon nanotube (MWCNTs): The CNTs were synthesized by the Chemical Catalytic Vapour Deposition (CCVD) which is made up of a vertical silica plug flow reactor inside a furnace. It is a modification of the chemical vapour deposition (Anreddy *et al*., 2010). The furnace is connected to a swirled coiled mixer with a supply of gas system of valves

and rotameters. The upper part of the reactor is connected to a condenser which leads to two delivery cyclones where the CNTs are collected. The system is also connected to a temperature regulator and a pressure controller. The valves control the flow of gases into the reactor. The CNTs were produced according to Yah *et al.* (2011) and viewed using the JEOL JEM-100S Transmission Electron Microscopy (TEM).

Functionalization of CNTs with sulphuric acid and nitric acid: The pristine MWCNTs were treated with hydrochloric acid, to remove impurities. One gram of MWCNTs was placed in a 500 mL round-bottom flask and 200 mL of HCL (30%) was added. The mixture was stirred using magnetic stirrer for 2 h, then diluted in water, filtered washed with deionised water and then dried overnight in a vacuum at 40°C to remove the iron impurities.

To functionalize the purify CNTs, 0.1 g of the purified MWCNTs were dispersed in 200 mL of acid (mixture of sulphuric acid 95% and nitric acid 95% of ratio 3:1) in a 500 mL round bottom flask equipped with a condenser. The dispersion was kept differently for 4 h at 100°C, 24 h at 50°C and 96 h at Room Temperature (RT). The resulting dispersion was diluted in water to neutral pH, filtered and the sample was dried in a vacuum at 40°C overnight. The modified CNTs (termed f-MWCNTS) were quantitatively analyzed by titration to determine the carboxylic acid (−COOH) concentrations on the surface of treated CNTs. The f-MWCNTs were added into a 25 mL 0.04 M NaOH solution and stirred for 48 h to allow the solid CNT material to equilibrate with the NaOH solution. The mixture was then titrated with a 0.04 M HCl solution to determine the excess NaOH in the solution and the concentration of the carboxylates on CNTs.

Functionalization of CNTs with Aspartic acid: Approximately 0.15 g of MWCNTs were dispersed in a mixture of 3 g of Aspartic acid and 15 mL of N, N-Dimethyl Formamide (DMF) in a round-bottom flask of 250 mL equipped with a condenser and the reaction was controlled to 220°C for 6 h. After filtration, the solid was washed with water to neutral pH. The yield obtained was 183 mg.

Using titration formula:

$$Y = 1\text{-}0.04\ X \quad (1)$$

where, Y = mmol of COOH on the surface of CNTs, X = The volume of HCl in mL.

The 1H NMR (29) analyses with D_2O +NaOH showed CH_2-COOH pick at chemical shift (3-2.3) expected. The TEM analysis were done according to the microscopic image obtained in Fig. 4 with nanotubes structure at d_0 = 60 nm.

Functionalized carbon nanotubes (f-CNTs)-folic acid conjugates

A: f-CNTs (H_2SO_4+HNO_3 at 100°C) bound folic acid: Approximately 100 mg of f-CNTs (prepared at 100°C) representing 0.38 mmol COOH was dispersed in 5 mL of DMF and 11.6 mg (0.114 mmol) of 3-Dimethylamino-1-Propylamine (DMP) representing 30% of molecular rate was dissolved in 4 mL of DMF. After nitrogen flashing, the dispersion and the solution were mixed together in a round bottom flask, stirred at 50°C. While solution was still stirring, 75 mg (0.32 mmol) of 2-(1H-benzotriazol-1-yl)-1,1,3,3-tetramethyluronium fluorophosphates (HBTU was added and the pH was controlled to 7 using the triethylamine (TEA) dropwise. After 24 h of reaction, a solution of 141 mg (0.32 mmol) 20% excess of folic acid in 10 mL of DMF was prepared for 1 h and was added in the main solution. Stirring was maintained for 6 h while the pH was kept to 7 with TEA. The solid was collected by filtration and washed several times with Tetramethylurea (TMU) to remove the excess FA and acetone. The solid was dried and kept in the desiccators.

B: f-CNTs (Aspartic acid)bound folic acid (f-CNTs-DMP (40)-FA (60)): Also 100 mg of f-CNTs representing 40 mg (0.88 mmol) of CNT-COOH was dispersed in 5 mL of DMF and 36 mg (0.352 mmol) of 3-dimethylamino-1-propylamine (DMP) (40%) was dissolved in 4 mL of DMF. After nitrogen flashing, the dispersion and the solution were mixed together in a round-bottom flask, stirred at 50°C. During stirring, 206 mg (0.88 mmol) of 2-(1H-benzotriazol-1-yl)-1,1,3,3-tetramethyluronium fluorophosphates (HBTU) predissolved in 3 mL DMF was added dropwise and the pH was neutralised to 7 using the Triethylamine (TEA). After 2 h of reaction, a solution of 303 mg (0.7 mmol) of FA in 15 mL of DMF was prepared for 1 h and was added into the main solution. Stirring continued for 6 h while the pH was kept at 7 with TEA. The solid was washed several time with Tetramethylurea (TMU) and filtered to remove the excess FA and acetone. The solid was dried and kept in the desiccators.

The ^{1}H NMR spectra and the Solid-state Infrared (IR) analysis: The ^{1}H NMR spectra were obtained at 300 and 400 MHz in DO_2 solution. The chemical shifts, δ in ppm

were referenced against sodium 3-(trimethylsily)-2, 2, 3, 3-d_4 propionate. The pH values of the sample in DO_2 solution were adjusted to 10-11 by adding sodium hydroxide in order to eliminate potential protonation effect. The Solid-state Infrared (IR) spectra were recorded on KBr pellets over the region of 4000-6000 cm^{-1}. The attention was turned only on the significant bands. Samples for analysis were dried using the Abderhalden apparatus and calcium chloride was done on a HITACHI 2000 spectrometer, at a scan speed of 400 nm min^{-1}.

RESULTS AND DISCUSSION

Synthesis of carbon nanotubes: The analysis of the Chemical Vapor Deposition (CVD) product by TEM showed MWCNTs with outer diameter (d_0) of 20 nm and an inner diameter (d_i) of 10 nm as shown in Fig. 1. The MWCNTs were similar to those earlier produced and reported by Iyuke *et al.* (2009) and Mohamed and Kou, 2011 where the optimal temperature for production was found at 900^0C with similar diameter. The results were dissimilar from those produces by Mamba *et al.* (2010) where they found MWCNTs as straight bundles of uniform lengths, each bundles consisting of numerous closely packed MWCNTs ropes with no indication of surface modifications.

The CNTs found could have a variety of applications because of their novel structure, especially the small size and remarkable mechanical, thermal and electrical properties (Zambri *et al.*, 2011). Small-diameter MWCNTs have ability to display enhanced reactivity relative to larger-diameter nanotubes, due to increased curvature strain. However, because of their novel structure of elemental carbon, CNTs are insoluble in all organic solvents (Kostarelos, 2003).

Covalent functionalization of carbon nanotubes

Functionalization of CNTs with concentrated nitric acid and sulfuric acid: (a) The MWCNTs were functionalized with H_2SO_4/HNO_3 in mol ratio of 3:1 at 100, 50°C and Room Temperature, respectively (RT). The TEM analysis of the f-MWCNTs showed variation at 100°C with outer diameter (d_0) = 20 nm and the inner diameter (d_{in}) = 12 nm (Fig. 2) while at 50°C d_o= 30 nm (Fig. 3) and at Room Temperature (RT) d_0 = 80 nm and d_{in}= 40 (Fig. 4). In order to evaluate the variation of the size of f-CNTs in terms of temperature, a graph of diameter versus temperature was plotted as shown in Fig. 5. The water solubility of f-CNTs was decreasing from 100°C to RT especially from pH = 9 and above.

The analysis of ^{1}H NMR Spectra 1, 2, 3 done for f-CNTs obtained at 100°C, 50°C, RT respectively showed

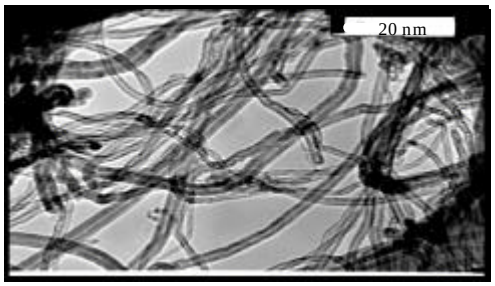

Fig. 1: MWCNTS microscopic image (TEM)

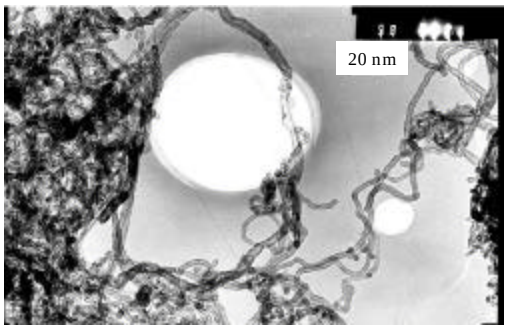

Fig. 2: f-CNTs (H2SO4/HNO_3 at 100°C) microscopic image

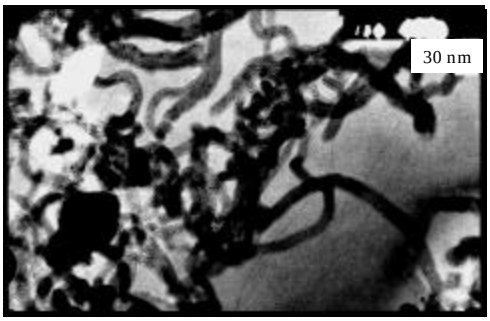

Fig. 3: f-CNTs (H_2SO_4/HNO_3 at 50°C) microscopic image

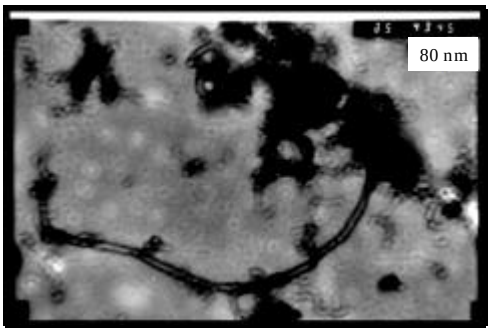

Fig. 4: f-CNTs (H_2SO_4/HNO_3 at RT) microscopic image

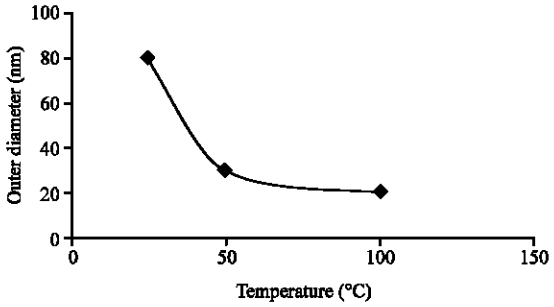

Fig. 5: Size of CNTs versus temperature

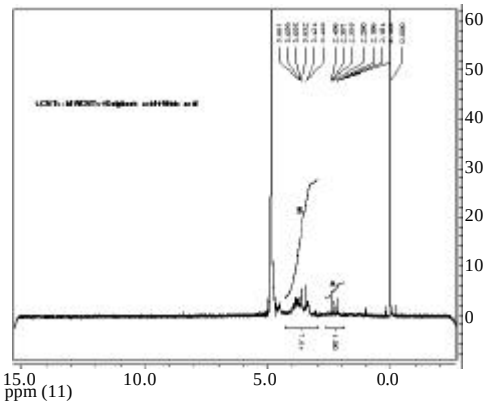

H NMR Spectra 1: f-CNTs: MWCNTs in H_2SO_4/ HNO_3 at 100°C

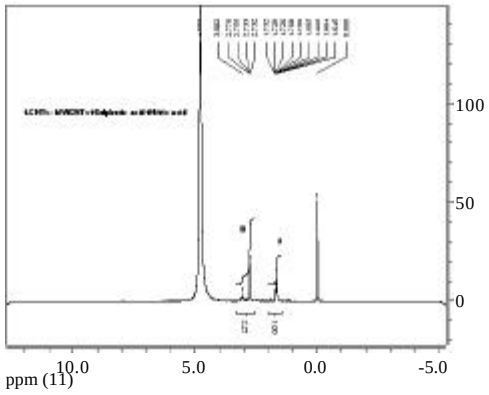

^{1}H NMR Spectra 2: f-CNTs: MWCNTs in H_2SO_4/HNO_3 at 50°C

peaks A and B in chemical shift δ/ppm (1.5-2.5) for $-CH_2COOH$ and (2.7-3.7) for $-CH_2OH$. In order to calculate the quantity of COOH and OH, the integration of peak A ($-CH_2COOH$) corresponding to 1 mol and was used as reference to evaluate the peak B ($-CH_2OH$). After calculation, the following results were obtained:

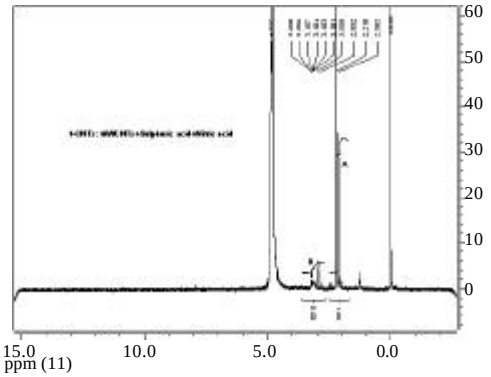

^{1}H NMR Spectra 3: f-CNTs: MWCNTs in H_2SO_4/HNO_3 at RT

- The integration of peaks A and B in ^{1}H NMR Spectra 1 for f-CNTs (100°C) shows after evaluation that 1 mol of COOH adsorbed on the surface of MWCNTs, corresponded to 7.54 moles of OH
- The integration of peaks A and B in ^{1}H NMR Spectra 2 for f-CNTs (50°C) shows after evaluation showed 1mol of COOH absorbed on the surface of MWCNTs, corresponded to 2.27 mol of OH
- The integration of peaks A and B in ^{1}H NMR Spectra 3 for f-CNTs (RT) after evaluation showed 1 mol of COOH absorbed on the surface of MWCNTs, corresponded to 0.08 mol of OH

A sample of 200mg of f-CNTs was used for titration to evaluate the quantity of COOH in mmol incorporated on the surface of f-CNTs which through the mol ratio COOH/OH was calculated from different ^{1}H NMR spectra. The integration was used to calculate the quantity of OH in mmol incorporated on the surface of f-CNTs. The experimental data from titration was used through the formula Y = 1-0.04 X to complete Table 1. The results in Table 1 were used to plot fraction of incorporation of COOH and OH versus the temperature as shown in Fig. 7 and the mol ratio COOH/OH versus the temperature as shown in the Fig. 8.

Different peaks including A, B, C, D and E were shown in the infrared (IR) investigation as presented in Fig. 6.

- A:O-H stretch (3331.44 cm and 3334.86 cm) intermolecular hydrogen bonded B:C-H stretch; (2892.90 and 2902.20 cm)
- C:C = O, stretch; (1693.04 and 1716.56 cm)
- D:C-O (1158.92-1028.01 cm^{-1}) and (1156.39-1.1030.67 cm^{-1}), stretch
- E: Ring C = C, bend (663.67-574.56 cm^{-1}), this confirm the CNTs the graphene structure with sp^2-bond carbon

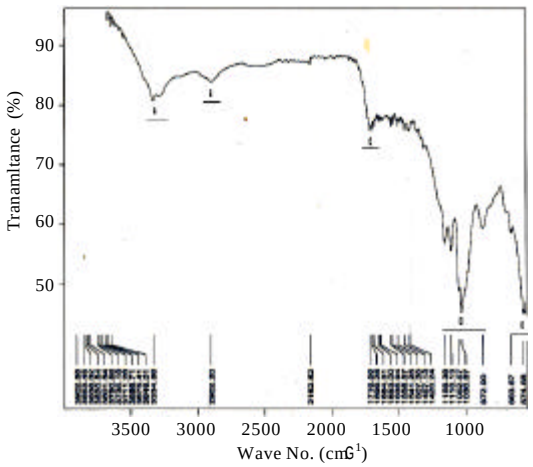

Fig. 6: Infrared Peaks of f-CNTs (H_2SO_4/HNO_3) at 100°C

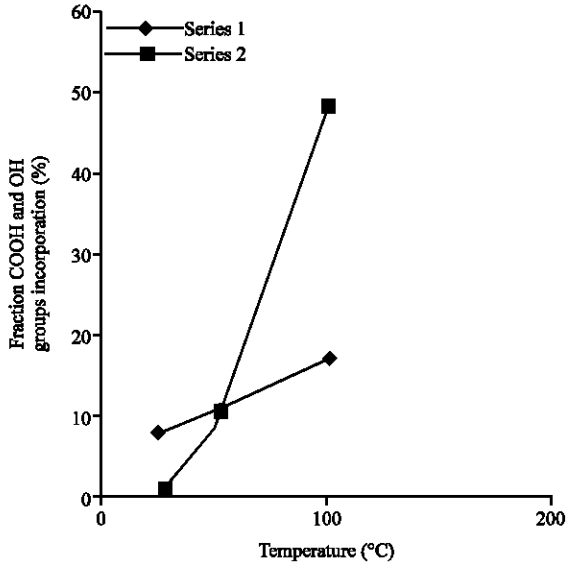

Fig. 7: Fraction of COOH and OH group incorporation versus temperature

The results in Fig. 5 are elaborated from the TEM analyses in Fig. 2-4 which showed increase in size of nanotubes which were relative to decrease in temperature. This might have been due to self-diffusion of molecules inside of CNTs thereby allowing the CNTs to form a well-ordered nanoporous membrane (Casavant *et al*., 2003; Hinds *et al*., 2004) which can be incorporated in a macroscopic structure (Srivastava *et al*., 2004) for separation devices. The study of self-diffusivity can explain the non parabolic influence of nanotube sizes and temperature. Jobic and co-workers had examined this

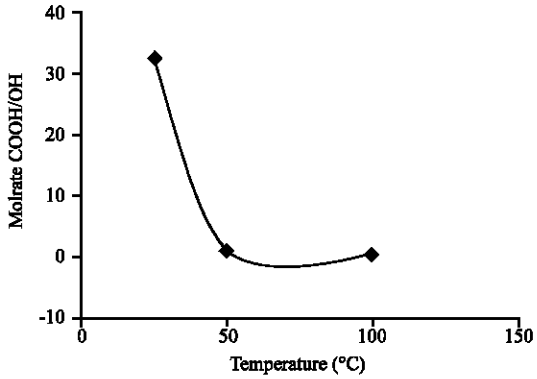

Fig. 8: Mol rate COOH/OH versus temperature

Table 1: Fraction incorporation of COOH and OH on the surface of CNTs with variable temperature

T°C	25°C (RT)	50°C	100°C
Mass of f-CNTs	200 mg	200 mg	200 mg
nH[2]: COOH	1	1	1
nH: OH	0.08	2.27	7.54
X[3] (mL)	16 (mL)	13 (mL)	6 (mL)
Y[4] (mmol)	0.36 (mmol)	0.48 (mmol)	0.76 (mmol)
COOH incorp. (%)	8.1	10.8	17.1
% OH incorp.	0.25	9.9	48.7

[2]nH: Number of Hydrogen atom, [3]X: The volume of HCl in mL, [4]Y: The quantity of COOH in mmol incorporated on the surface of f-CNTs

effect in more detail for diffusion (Jobic *et al*., 2009) using molecular dynamics simulations. They termed this behaviour the "Levitation effect". If the guest molecule fits perfectly in the window of the zeolite, the molecule appears to be floating; increasing or decreasing the diameter of the guest molecules as well as reducing the diffusion coefficient. This effect is temperature dependent (Derouane *et al*., 1988). A similar effect has been observed by Cannon and Hess (2010) for carbon nanotubes.

With regard to Fig. 5, the self-diffusivity was subsequently increasing with decreasing of temperature. Since the self-diffusion explains the incorporation of guest molecule in CNTs through nanoporous membrane, the diameter of CNTs has to increase in the tendency where the self-diffusion will increase. According to the objective of the study, attention was given to the trend where the surface adsorption (surface phenomenon) was possible, rather than where absorption was evident. The increase temperature which led to decrease in diameter, resulted in higher collision frequencies and faster motion. This enhances the particle probability to bond folic acid. The f-MWCNTs at 100°C were selected, due to their small size and the adsorption capabilities.

The ^{1}H NMR Spectra 1, 2 and 3 were obtained with D_2O as solvent. Therefore COOH and OH groups directly attached on the surface of CNTs were shifted in δ/ppm

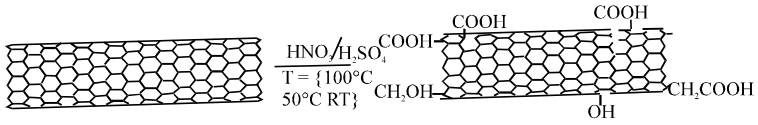

Scheme 1: f-CNTs (H_2SO_4/HNO_3) structure

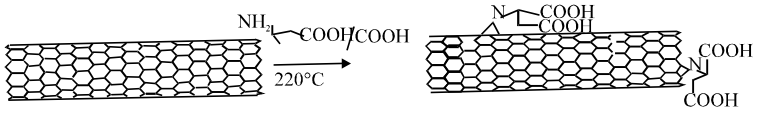

Scheme 2: f-CNTs (aspartic acid) structure

(4.5-5.5) for D_2O peaks. The ^1H NMR analysis for all f-CNTs made at different temperatures (100, 50°C and RT) shown the presence of CH_2COOH and CH_2OH due to the fact that amorphous carbon was removed purification by HCL (Monthioux *et al*., 2010).

In addition, the infrared analysis from Fig. 6 and the ^1H NMR Spectra 1, 2 and 3 have confirmed that f-CNTs were produced and the entire MWNTs was covered with CH_2OH, CH_2COOH, OH and COOH as shown in Scheme 1.

In comparison with the result from Fig. 7 and 8, it was found that both fractions of OH and COOH incorporation in f-CNTs were increasing with increasing temperature. At room temperature, the fraction of OH group incorporation was much neglected and the mol ratio COOH/OH was 32.4, these were rapidly reduced to 1.1 at 50°C and sharply down to 0.35 at 100°C. This shows that when working at room temperature or below there is possibility of getting f-CNTs covered only with COOH. It was found that f-CNTs at 100°C were more soluble than at RT and 50°C due to high presence of OH groups on the CNTs surfaces. Thus, the abundance of OH and COOH groups on the surface will facilitate more covalent attachment to polymers or drugs according to their different electronegativities. This granted the f-CNTs made at 100°C to be more useful than those made at low temperatures. The scope of this reaction was very broad and produces f-CNTs that possess high solubility in a wide range of different solvents. This was preferentially selected for the next phase of the drug binding to carbon nanotubes.

Where Series 1: Fraction incorporation of carboxyl group (COOH) on the surface of CNTs and Series 2: Fraction incorporation of phenol group (OH) on the surface of CNTs.

Functionalization of CNTs with Aspartic acid: The functionalized carbon nanotubes (f-CNTs) were also obtained by heating MWNTs with aspartic acid an amino acid in DMF at 220°C. This resulted to the structure as shown in Scheme 3. The results of f-CNTs by aspartic are shown in Fig. 9 where 183 mg of f-CNTs by aspartic acid were soluble in water at pH of 10.

The ^1H NMR Spectra 4 showed peaks A in chemical shift (δ/ppm) 3.050-2.200 for $-CH_2COOH$ and B in chemical shift (δ/ppm) 4.40-4.70 for = N-CH CH_2 $(COOH)_2$ as expected. The different peaks was obtained from infrared (IR) investigation (A, B, C, D, E, F and G) are shown in Fig. 10.

- A: N-H stretch, at 3331.44 cm^{-1}; B: C-H stretch in the region 3015.95-2902.20cm^{-1} C: Overtone region usually contains a prominent band in the region 2337.23-2119.11cm^{-1} D: C = O bond stretch, at 1738.63 cm^{-1}; E: C-N stretch, at 1436.30 cm^{-1} F: C-O (acetate) stretch, in the region 1228.93-1216.70 cm^{-1}; G: O-H out of plane bend, 1011.82-912.05 cm^{-1}

Using the titration formula Y = 1-0.04 X (Y: quantity of COOH in mmol incorporated on the surface of f-CNTs and X: volume of HCl in mL) when working with 200 mg of f-CNTs 0.88 mmol of COOH corresponding to 20% of COOH was incorporated on the surface of CNTs after neutralization with excess NaOH and 3 mL of HCl. The carboxyl group incorporated in the f-CNTs was intended to be bound with the solubilizing group and the drug. The quantity of the solubilizing group and drug were evaluated with 20% of fraction of COOH-f-CNTs at pH of 10. The TEM analysis showed f-CNTs-aspartic acid diameter at 60 nm which was larger than the diameter obtained for MWNTs in sulfuric and nitric acids at 100 and 50°C and to a lesser extend at RT. According to the findings from Fig. 5, the diameter was decreasing with increase in temperature which was similar to those earlier reported by Hunger *et al*. (2002), Jakobtorweihen *et al*. (2006). The investigation of peaks in ^1H NMR Spectra 4 and infrared (IR) as shown in Fig. 10 which confirm the structure elaborated in Scheme 2.

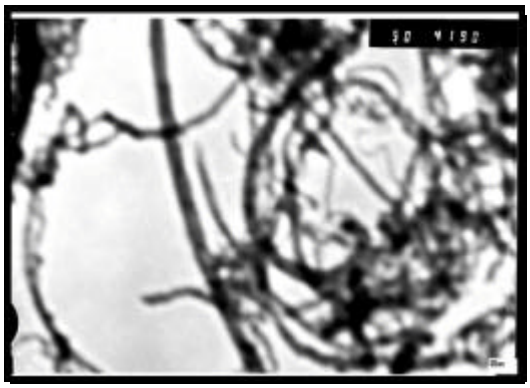

Fig. 9: f-CNTs (MWNTs +Aspartic acid in DMF at 220°C)

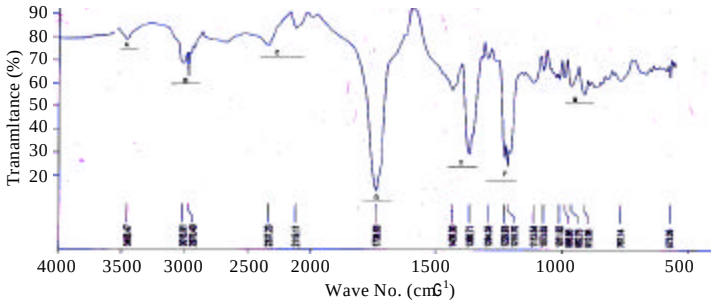

Fig. 10: IR f-CNTs (aspartic acid)

Overall, the use of strong acid and amino acid to functionalize the carbon nanotubes generates carboxylic groups (Scheme 1, 2) which increase their dispersibility in aqueous solutions (Tasis *et al*., 2006; Kim *et al*., 2007). Solubility under physiological conditions is a key prerequisite to make CNT biocompatible which can be linked to a wide variety of active molecules.

Functionalized carbon nanotubes (f-CNTs) bound Folic acid conjugates: The folic acid was functionalized with the MWCNTs by the aid of 3-dimethylamino-1-propylamine (DMP) as a strong base. This gave the amino group a positive charge enabling the FA to bind. This was similar to those reported by Zeng *et al.* (2006) were they prepared functionalized CNTs with biodegradable poly (e-caprolactone) (PCL). They found that the presence of CNTs did not affect the biodegradability of PCL. From HNMR results it was found that FA was attached to surface of the MWCNTs. Furthermore functionalized CNT-PCL polymer matrix could display enormous potential as a structural support material in tissue engineering.

f-CNTs (H_2SO_4+HNO_3 at 100°C) bound folic acid conjugates: The estimation of the percentage of -COOH in f-CNTs was proved by the titration. The f-CNTs was achieved by the reaction between –COOH and NH_2 via the coupling agent 0-benzotiazol-1-yl-tetramethylurorium hexafluorophosphate (HBTU). Thus, the coupling led to the yield of 163 mg f-CNT-FA similar to the chemical structure presented in Scheme 3. The TEM analysis of f-CNTs (H_2SO_4+HNO_3 at 100°C) bound folic acid conjugates are shown in Fig. 11 with d_0 = 50 nm and d_{in} = 20 nm and soluble at pH 6-7. The ^{1}H NMR Spectra 5 were similar to peaks shift shown in Scheme 3 as illustrated in Table 2.

With the size of 50 nm as outer diameter and 20 nm as inner diameter the conjugate can be easily tracked into the cytoplasm and the nucleus. With regard to the ^{1}H NMR Spectra 5, the fraction of incorporation of folic acid was calculated by using the integration of A that is 1 and the sum of integration of aromatic group E, F and G which is 1.64. With 30% of DMP and 70% of folic acid, the mol ratio was 3/7 and the number of H expected was 20 H for A and 35H for the sum of E, F and G as it is shown in the structure (Scheme 3). Referring to A as 20H calculated with integration 1, the sum of E, F and G with integration of 1.64 gave 32.8H calculated which corresponded to 94% incorporation.

f-CNTs (Aspartic acid) bound folic acid conjugates: The estimation of the percentage of –COOH in f-CNTs was also evaluated by the titration which was achieved by the

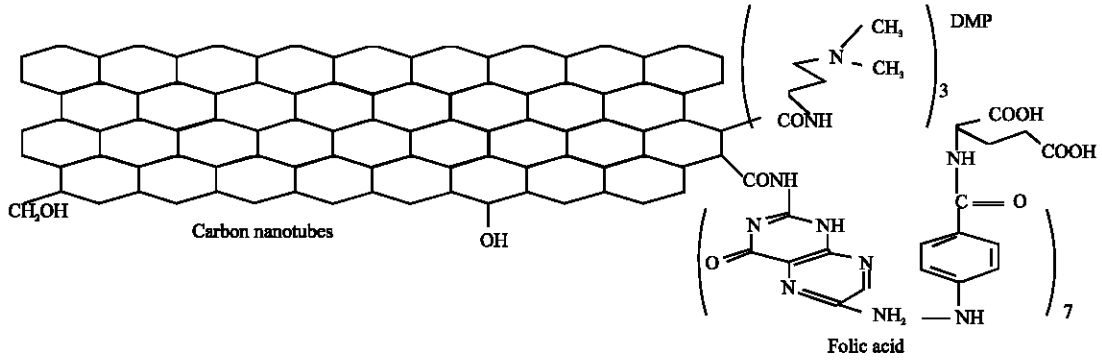

Scheme 3: f-CNTs (H_2SO_4/HNO_3)-DMP (30)-FA (70) Structure

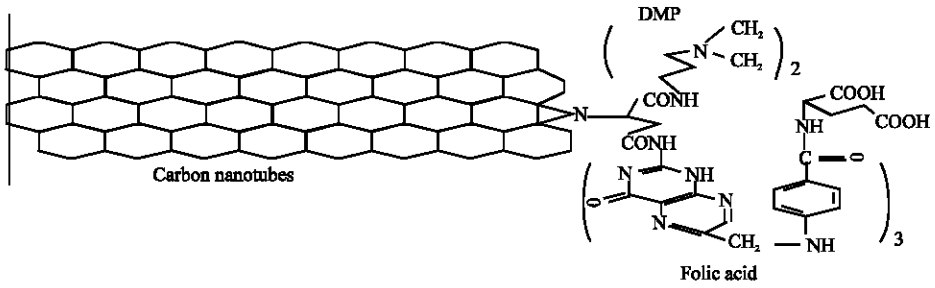

Scheme 4: f-CNTs (Aspartic acid)-DMP (40)-FA (60) Structure

Fig. 11: f-CNTs (H_2SO_4/HNO_3)-FA

Table 2: HNMR spectra of f-CNTs (H_2SO_4/HNO_3)-FA

Chemical shift δ/ppm	^{1}H NMR peacks identification	Assignment
8.60-6.75	G, F, E	CH Aromatic
4.85 -4.28	C	CH Asp, CH Folic acid and CH_2OH
3.25-2.75	D	$-CONHCH_2$, $NHCH_2$, $-CH_2NH$
2.25-1.8	B	$-CH_2COOH$, CH_2CONH, $NH(CH_3)_2$
1.8-1.7	A	$COOHCH_2CH_2CH$, $CH_2CH_2CH_2$

^{1}Y is the quantity of COOH in mmol incorporated on the surface of f-CNTs and X is the volume of HCl in mL

Table 3: HNMR data f-CNTs (aspartic acid)-DMP (40)-FA (60)

Chemical shift δ/ppm	^{1}HNMR peaks identification	Assignment
8.7-6.8	G, F, E	CH Aromatic
4.7-4.25	D	CH Asp, CH Folic acid
3.2-2.9	C	$-CONHCH_2$, $NHCH_2$, $CH_2NH(CH_3)_2$
2.3-1.8	B	$-CH_2COOH$, CH_2CONH, $COOHCH_2CH_2CH$
1.8-1.7	A	$CH_2CH_2CH_2$

^{1}Y is the quantity of COOH in mmol incorporated on the surface of f-CNTs and X is the volume of HCl in mL

reaction between –COOH and NH_2 via the coupling agent 2-(1H-benzotriazol-1-yl)-1,1,3,3-tetramethyluronium fluorophosphates (HBTU). With the objective to raise the water solubility of f-CNTs, 40% of –COOH was evaluated using attached DMP as the solubilizing group. The folic acid was used in excess with the objective to complete all the 60% of -COOH that did not react with DMP. The result f-CNTs (Aspartic acid) bound folic acid conjugate yielded 231 mg and the chemical structure is presented in Scheme 4. The TEM analysis is shown in Fig. 12 having diameter of 170 nm. The product was soluble at pH of 6-7.

The ^{1}H NMR Spectra 6 showed all expected chemical bands as illustrated in Table 3. This therefore, confirms the reversible attachment between f-CNTs with DMP and folic acid via amid bond formation. To calculate the fraction incorporation of folic acid, the integration of peak A evaluated to 1 was chosen as reference and corresponded to 4 H as expected and the integration of aromatic peaks (E, F, G) evaluated to 3.8 was calculated 15.2 H while the expected was 15 H as shown in Scheme 4 and then the fraction incorporation of folic acid was 101.3%. The error was 1.3%.

The f-CNTs-drug conjugate from aspartic acid (Fig. 12) showed the dark spot spread along the nanotubes while Fig. 11 related to the f-CNTs of conjugate made from H_2SO_4/HNO_3 at 100°C also dark spot

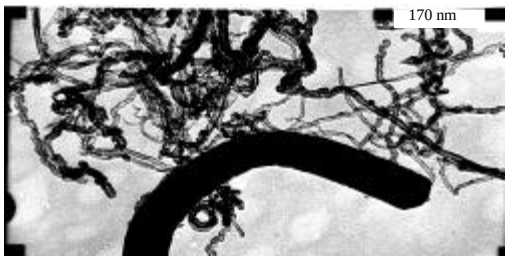

Fig. 12: f-CNTs (Aspartic acid)-DMP (40)-FA (60) microscopic image

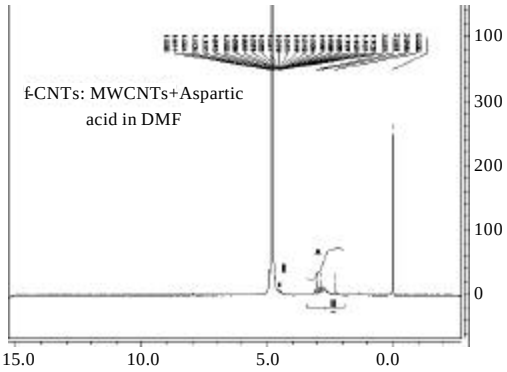

^{1}H NMR Spectra 4: f-CNTs: MWCNTs+Aspartic acid in DMF at 230°C.

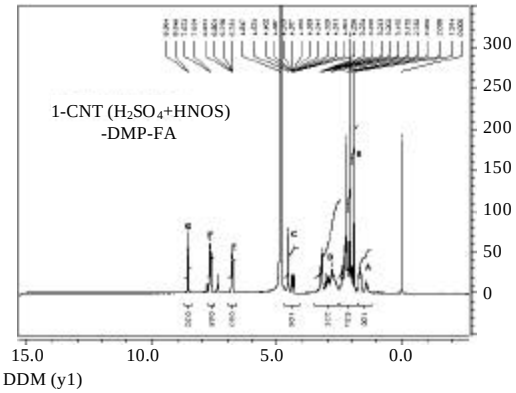

^{1}H NMR Spectra 5: f-CNTs (MWCNTs+H_2SO_4+HNO_3)-DMP (30)-FA (70) 94% FA incorporation

at the end cap. The incorporation of COOH (17.1%) in f-CNTs with H_2SO_4/HNO_3 at 100°C (Table 1) was lesser than the one (20%) in f-CNTs with aspartic acid.

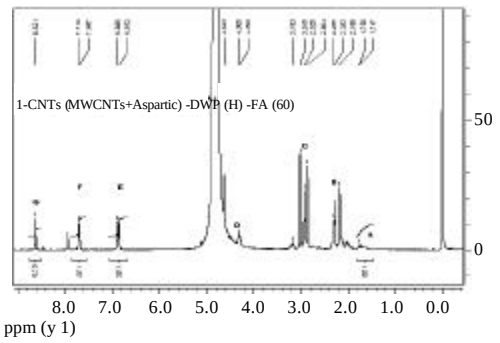

^{1}H NMR Spectra 6: f-CNTs (MWCNTs+Aspartic Acid)-DMP(40)-FA(60) Incorporation FA 101,3%

CONCLUSION

The carbon nanotubes, due to its small size were synthesised as drug carrier target. The covalent functionalization was developed on the surface of MWCNT. The carboxyl groups reacted with HBTU as coupling agent DMP amines in one part and folic acid in other. The formation of CONH as bioreversible bond between the f-CNTs and folic acid was determined by ^{1}H NMR and IR. The soluble f-MWCNTs TEM structures were conserved within the diameter range of 50 to 170 nm. The phenol (OH) and carboxyl (COOH) groups were attached on the surface of CNT making the rate COOH/OH to decrease with increasing temperature. The f-CNT covered surface with OH and COOH was more water soluble than the f-CNT covered COOH.

ACKNOWLEDGMENTS

The authors acknowledge the financial support from the National Research Foundation (NRF) under the NRF Focus Area: NRF Nanotechnology flagship programme, DST/NRF Centre of Excellence. The student bursaries provided by the Wits University are much appreciated.

REFERENCES

Alkhatib, M.F., M.E.S. Mirghani, I.Y. Qudsieh and I.A.F. Husain, 2010. Immobilization of chitosan onto carbon nanotubes for lead removal from water. J. Applied Sci., 10: 2705-2708.

Allen, T.M. and P.R. Cullis, 2004. Drug delivery systems: Entering the mainstream. Science, 303: 1818-1822.

Anreddy, R.N.R., N.R. Yellu, R.K. Devarakonda and H. Vurimindi 2010. *In vitro* toxicity of multi wall carbon nanoparticles on Hep G 32 liver cell lines. J. Pharmacol. Toxicol., 5: 146-151.

Cannon, J. and O. Hess, 2010. Fundamental dynamics of flow through carbon nanotube membranes. Microfluid. Nanofluid., 8: 21-31.

Casavant, M.J., D.A. Walters, J.J. Schmidt and R.E. Smalley, 2003. Neat macroscopic membranes of aligned carbon nanotubes. J. Applied Phys., 93: 2153-2156.

Derouane, E.G., J.M. Andre and A.A. Lucas, 1988. Surface curvature effects in physisorption and catalysis by microporous solids and molecular sieves. J. Catal., 110: 58-73.

Fekri, L., A. Jafari, S. Fekri, A. Shafikhani, M. Vesaghi and G. Behzadi, 2010. Comparison of synthesis and purification of carbon nanotubes by thermal chemical vapor deposition on the nickel-based catalysts: $NiSio_2$ and 304-Type stainless steel. J. Applied Sci., 10: 716-723.

Ferrari, M., 2005. Cancer nanotechnology: Opportunities and challenges. Nat. Rev. Cancer, 5: 161-171.

Hinds, B.J., N. Chopra, T. Rantell, R. Andrews, V. Gavalas and L.G. Bachas, 2004. Aligned multiwalled carbon nanotube membranes. Science, 303: 62-65.

Hunger, B., M. Heuchel, A.L. Clark and Q.R. Snurr, 2002. Characterization of acidic OH groups in zeolites of different types: An interpretation of NH_3-TPD results in the light of confinement effects. J. Phys. Chem. B., 106: 3882-3889.

Iyuke, S.E., T.A. Mamvura, K. Liu, V. Sibanda, M. Meyyappan and V.K. Varadan, 2009. Process synthesis and optimization for the production of carbon nanostructures. Nanotechnology, 20, 10.1088/0957-4484/20/37/375602

Jakobtorweihen, S., F.J. Keil and B. Smit, 2006. Temperature and size effects on diffusion in carbon nanotubes. J. Phys. Chem. B, 110: 16332-16336.

Jobic, H., B.J. Borah and S. Yashonath, 2009. Neutron scattering and molecular dynamics evidence for levitation effect in nanopores. J. Phys. Chem. B., 113: 12635-12638.

Kam, N.W.S., T.C. Jessop, P.A. Wender and H. Dai, 2004. Nanotube molecular transporters: Internalization of carbon nanotube-protein conjugates into Mammalian cells. J. Am. Chem. Soc., 126: 6850-6851.

Ke, G., W. Guan, C. Tang, W. Guan, D. Zeng and F. Deng, 2007. Covalent functionalization of multiwalled carbon nanotubes with a low molecular weight chitosan. Biomacromolecules, 8: 322-326.

Kim, S.N., J.F. Rusling and F. Papadimitrakopoulos, 2007. Carbon nanotubes for electronic and electrochemical detection of biomolecules. Adv. Mater., 19: 3214-3228.

Kostarelos, K., 2003. Rational design and engineering of delivery systems for therapeutics: Biomedical exercises in colloid and surface science. Adv. Colloid Interface Sci., 106: 147-168.

Mamba, G., X.Y. Mbianda, P.P. Govender, B.B. Mamba and R.W. Krause, 2010. Application of multiwalled carbon nanotube-cyclodextrin polymers in the removal of heavy metals from water. J. Applied Sci., 10: 940-949.

Mohamed, N.M. and L.M. Kou, 2011. Sandwich Growth of Aligned Carbon Nanotubes Array using Thermal Chemical Vapor Deposition Method J. Applied Sci., 11: 1341-1345.

Monthioux, M., P. Serp, E. Flahaut, C. Laurent and A. Peigney *et al*., 2010. Introduction to Carbon Nanotubes. In: Handbook of Nanotechnology, Bhushan, B. (Ed.). 3rd Edn., Springer-Verlag, Heidelberg, Germany, pp: 47-118.

Niyogi, S., M.A. Hamon, H. Hu, B. Zhao and P. Bhowmik *et al*., 2002. Chemistry of single-walled carbon nanotubes. Acc. Chem. Res., 35: 1105-1113.

Pantarotto, D., J.P. Briand, M. Prato and A. Bianco, 2004. Translocation of bioactive peptides across cell membranes by carbon nanotubes. Chem. Commun., 7: 16-17.

Pastorin, G., W. Wu, S. Wieckowski, J.P. Briand, K. Kostarelos, M. Prato and A. Bianco, 2006. Double functionalization of carbon nanotubes for multimodal drug delivery. Chem. Commun., 11: 1182-1184.

Pignatello, R., I. Toth and G. Puglisi, 2001. Structural effects of lipophilic methotrexate conjugates on model phospholipid biomembranes. Thermochim. Acta, 380: 255-264.

Pignatello, R., S.Guccione, S. Forte, C. Di Giacomo and V. Sorrenti *et al*., 2004. Lipophilic conjugates of methotrexate with short-chain alkylamino acids as DHFR inhibitors. Synthesis, biological evaluation and molecular modelling. Bioorg. Med. Chem., 12: 2951-2964.

Pouton, C.W. and L.W. Seymour, 2000. Key issues in non-viral gene delivery. Adv. Drug. Deliv. Rev., 46: 187-203.

Prato, M., K. Kostarelos and A. Bianco, 2008. Functionalized carbon nanotubes in drug design and discovery. Acc. Chem. Resi., 41: 60-68.

Quintana, A., E. Raczka, L. Piehler, I. Lee and A. Myc *et al*., 2002. Design and function of a dendrimer-based therapeutic nanodevice targeted to tumor cells through the folate receptor. Pharm. Res., 19: 1310-1316.

Rosca, I.D., F. Watari, M. Uo and T. Akasaka, 2005. Oxidation of multiwalled carbon nanotubes by nitric acid. Carbon, 43: 3124-3131.

Semwal, R., D.K. Semwal, R. Badoni, S. Gupta and A.K. Madan, 2010. Targeted drug nanoparticles: An emphasis on self-assembled polymeric system. J. Med. Sci., 10: 130-137.

Singh, M., S. Manikandan and A.K. Kumaraguru, 2011. Nanoparticles: A new technology with wide applications. Res. J. Nanosci. Nanotechnol., 1: 1-11.

Srivastava, A., O.N. Srivastava, S. Talapatra, R. Vajtai and P.M. Ajayan, 2004. Carbon nanotube filters. Nat. Mater., 3: 610-614.

Tasis, D., N. Tagmatarchis, A. Bianco and M. Prato, 2006. Chemistry of carbon nanotubes. Chem. Rev., 106: 1105-1136.

Vasir, J.K., M.K. Reddy and V.D. Labhasetwar, 2005. Nanosystems in drug targeting: Opportunities and challenges. Curr. Nanosci., 1: 47-64.

Warisnoicharoen, W., P. Hongpiticharoen and S. Lawanprasert, 2011. Alteration in enzymatic function of human cytochrome P450 by silver nanoparticles. Res. J. Environ. Toxicol., 5: 58-64.

Wong, J.M., 2005. Methotrexate in systemic lupus erythematosus. Lupus, 14: 101-105.

Wu, W., S. Wieckowski, G. Pastorin, C. Klumpp and M. Benincasa *et al*., 2005. Targeted delivery of amphotericin b to cells by using functionalized carbon nanotubes. Angew. Chem. Int. Ed., 44: 6358-6362.

Xie, J., N. Zang, M. Guers and V.K. Varadan, 2002. Ultraviolet-curable polymers with chemically bonded carbon nanotubes for microelectromechanical system applications. Smart Mater., 11: 575-580.

Yah, C.S., S.E. Iyuke, G.S. Simate, E.I. Unuabonah, G. Bathgate, G. Matthews and H.J.D. Cluett, 2011. Continuous synthesis of multiwalled carbon nanotubes from xylene using the swirled floating catalyst chemical vapor deposition Technique. J. Mater. Res., 26: 640-644.

Zambri, M.S.M., N.M. Mohamed and C.F. Kait, 2011. Preparation of electrochromic material using carbon nanotubes (CNTs). J. Applied Sci., 11: 1321-1325.

Zeng H.L., C. Gao and D.Y. Yan, 2006. Poly (ε-caprolactone)-functionalized carbon nanotubes and their biodegradation properties. Adv. Funct. Mater., 16: 812-818.

Zeng, L., L.B. Alemany, C.L. Edwards and A.R. Barron, 2008. Demonstration of covalent sidewall functionalization of single wall carbon nanotubes by NMR spectroscopy: Side chain length dependence on the observation of the sidewall sp^3 carbons. Nano. Res., 1: 72-88.